Liver X Receptor α–Induced Cannabinoid Receptor 2 Inhibits Ubiquitin-Specific Peptidase 4 Through miR-27b, Protecting Hepatocytes From TGF-β

Hong Min Wu, Tae Hyun Kim, Ayoung Kim, Ja Hyun Koo, Min Sung Joo, and Sang Geon Kim

Liver X receptor-alpha (LXRα) acts as a double-edged sword in different biological situations. Given the elusive role of LXRα in hepatocyte viability, this study investigated whether LXRα protects hepatocytes from injurious stimuli and the underlying basis. LXRα activation prevented hepatocyte apoptosis from CCl_4 challenges in mice. Consistently, LXRα protected hepatocytes specifically from transforming growth factor-beta (TGF-β), whereas LXRα deficiency aggravated TGF-β-induced hepatocyte injury. In the Gene Expression Omnibus database analysis for $LXR^{-/-}$ mice, TGF-β receptors were placed in the core network. Hierarchical clustering and correlation analyses enabled us to find cannabinoid receptor 2 (CB2) as a gene relevant to LXRα. In human fibrotic liver samples, both LXRα and CB2 were lower in patients with septal fibrosis and cirrhosis than those with portal fibrosis. LXRα transcriptionally induced CB2; CB2 then defended hepatocytes from TGF-β. In a macrophage depletion model, JWH133 (a CB2 agonist) treatment prevented toxicant-induced liver injury. MicroRNA 27b (miR-27b) was identified as an inhibitor of ubiquitin-specific peptidase 4 (USP4), deubiquitylating TGF-β receptor 1 (TβRI), downstream from CB2. Liver-specific overexpression of LXRα protected hepatocytes from injurious stimuli and attenuated hepatic inflammation and fibrosis. *Conclusion*: LXRα exerts a cytoprotective effect against TGF-β by transcriptionally regulating the CB2 gene in hepatocytes, and CB2 then inhibits USP4-stabilizing TβRI through miR-27b. Our data provide targets for the treatment of acute liver injury. (*Hepatology Communications* 2019;3:1373-1387).

The liver consists of hepatocytes (about 60%-80%) and nonparenchymal cells (20%-40%).[1] Hepatocyte injury generally precedes most of liver disease progression.[2] Repetitive hepatocyte injuries facilitate serious pathologic progression such as fibrosis in the liver.[3] A variety of stimuli on the liver promote oxidative stress responses, trigger hepatocyte death signaling pathways, and activate other types of cells.[4] Thus, strategies to preserve functional hepatocytes would contribute to finding ways to overcome more serious liver diseases.

Liver X receptors (LXRs) regulate lipid metabolism and inflammation.[5] LXRα is expressed primarily in liver, intestine, kidney, and adipose tissue,

Abbreviations: α-SMA, alpha-smooth muscle actin; ALT, alanine aminotransferase; AML12, alpha mouse liver 12; APAP, acetaminophen; ASO, antisense oligonucleotide; AST, aspartate aminotransferase; CB2, cannabinoid receptor 2; DEG, differentially expressed gene; GEO, Gene Expression Omnibus; LV-LXRα^{alb}, albumin promoter–driven lentiviral LXR-alpha; LXR, liver X receptor; LXRα, liver X receptor-alpha; LXRE, LXR-response element; miR, microRNA; mRNA, messenger RNA; PKA, protein kinase A; RT-PCR, reverse-transcription polymerase chain reaction; siRNA, small interfering RNA; TβRI, transforming growth factor-beta receptor 1; TGF-β, transforming growth factor-beta; TUNEL, terminal deoxynucleotidyl transferase–mediated deoxyuridine triphosphate nick-end labeling; USP4, ubiquitin-specific peptidase 4; WT, wild type.

Received November 2, 2018; accepted July 13, 2019.

Additional Supporting Information may be found at onlinelibrary.wiley.com/doi/10.1002/hep4.1415/suppinfo.

Supported by the National Research Foundation of Korea (NRF) grant funded by the Korea government (MSIP) (NRF-2018R1A2-A1A05078694) to S.G.K.

Some of the data in this manuscript were presented at the 52nd European Congress of the European Societies of Toxicology in Seville, Spain (2016), and the 12th International Conference and 5th Asian Congress on Environmental Mutagens (ICEM-ACEM) in Incheon, Korea (2017).

whereas LXRβ is ubiquitously distributed.[5] LXRα appears to be more important in cholesterol and lipid metabolism in liver biology.[6] Excessive activation of LXRα augments triglyceride accumulation in the liver and causes lipotoxicity in association with steatosis and hypertriglyceridemia. Because LXRα is the major regulator of fatty acid biosynthesis in the liver,[7] numerous studies have focused on the deleterious effect of LXRα hyperactivation. However, the effect of LXRα on hepatocyte viability in metabolic disorders is controversial, implying that LXRα may act as a double-edged sword.

Because little is known on the role and mechanism of LXRα in hepatocyte viability in different biological situations, this study investigated whether LXRα protects hepatocytes from toxicant challenge, and if so, what the regulatory basis is. Here, we report the beneficial effect of LXRα on hepatocytes in association with the inhibition of transforming growth factor-beta (TGF-β) signaling. Specifically, we identified the transcriptional role of LXRα for cannabinoid receptor 2 (CB2) expression. In human liver specimen analysis, we verified paralleled decreases of LXRα and CB2 in patients with septal fibrosis and cirrhosis as compared with patients with portal fibrosis. To strengthen the role of CB2 in hepatocytes, we used a macrophage depletion model. Moreover, we discovered microRNA 27b (miR-27b) as an inhibitor of ubiquitin-specific peptidase 4 (USP4) and confirmed that miR-27b levels decreased in patients as liver fibrosis worsened and positively correlated with CB2 levels. Finally, the hepatocyte-specific LXRα overexpression technique was used to validate the effect of LXRα on hepatocyte protection.

Methods

MATERIALS

GW3965 (for cell-based assays), propidium iodide, and MG132 were provided from Sigma-Aldrich (St Louis, MO). Transforming growth factor-beta 1 (TGF-β1) was purchased from Humanzyme (Chicago, IL), whereas fluorescein isothiocyanate–annexin V was from BD Biosciences (San Jose, CA). GW3965 (for the *in vivo* experiment), SR144528, and SB525334 were supplied from Cayman Chemical (Ann Arbor, MI). JWH133 was provided from Tocris Bioscience (Bristol, United Kingdom). Clodronate liposome was purchased from FormMax (Sunnyvale, CA). mTNF-α was supplied from R&D Systems (Minneapolis, MN), and horseradish peroxidase–conjugated goat antirabbit and goat antimouse immunoglobulin Gs were from Zymed Laboratories (San Francisco, CA). Antibody information is provided in Supporting Table S1.

HUMAN LIVER SAMPLES

Human liver specimens were provided from the Asan Medical Center (Seoul, Korea) between 2006 and 2009. All of the procured specimens received proper patient consent with approval. Details are found in the online Supporting Information.

ANIMAL TREATMENTS

All animal studies were approved and conducted under the guidelines of the Institutional Animal Care and Use Committee at Seoul National University. Details are in the online Supporting Information.

View this article online at wileyonlinelibrary.com.
DOI 10.1002/hep4.1415

Potential conflict of interest: Nothing to report.

ARTICLE INFORMATION:

From the College of Pharmacy and Research Institute of Pharmaceutical Sciences, Seoul National University, Seoul, Korea.

ADDRESS CORRESPONDENCE AND REPRINT REQUESTS TO:

Sang Geon Kim, Ph.D.
College of Pharmacy, Seoul National University
1 Gwanak-ro, Gwanak-gu
Seoul 08826, South Korea
E-mail: sgk@snu.ac.kr
Tel.: +822-880-7840

TARGET GENE DELIVERY

Albumin promoter–driven lentiviral LXRα viruses were administered to LXRα$^{-/-}$ mice through the tail vein. Details are in the online Supporting Information.

STATISTICS

Data were shown as the mean ± SEM, and statistical significance was assessed using two-tailed Student *t* test. Coefficients of correlation (*r*) were determined by the Pearson analysis, and statistical calculations were performed using SPSS 22.0. The criterion for statistical significance was set at $P < 0.05$.

See the Supporting Information for additional information.

Results

ROLE OF LXRα IN LIVER CELL VIABILITY AGAINST TOXICANT

First, to understand the relevance of LXRα and hepatocyte viability, we tested the effect of LXRα agonist GW3965 on the liver of mice challenged with a single dose of CCl_4. GW3965 protected liver from toxicant, as evidenced by changes in terminal deoxynucleotidyl transferase–mediated deoxyuridine triphosphate nick-end labeling (TUNEL)-positive hepatocytes, improvements in histopathological assessments, and cell viability biomarkers (Fig. 1A). pCREB was selected as a marker for hepatocyte viability because of its association with protection of hepatocytes from harmful stresses (e.g., endoplasmic reticulum stress, oxidative stress).[8,9] The hepatocyte-protective effect of LXRα was verified by blood biochemical analyses (Fig. 1B, left) and decreased transcript levels of inflammatory markers in the liver (Fig. 1B, right). Next, LXRα$^{-/-}$ mice and age-matched wild-type (WT) controls were used to assess the functional role of LXRα in liver injury. Quantitative reverse-transcription polymerase chain reaction (RT-PCR) assays confirmed the LXRα gene (*Nr1h3*) knockout (Supporting Fig. S1A). GW3965 treatment decreased serum alanine aminotransferase (ALT) activity and hepatic messenger RNA (mRNA) level of bcl-2-associated X protein (*Bax*) in CCl_4-treated WT mice but not in the corresponding LXRα$^{-/-}$ mice (Supporting Fig. S1B), confirmative of liver protection by LXRα.

We also evaluated the degree of liver injury in a model of multiple CCl_4 injections. Four weeks of CCl_4 treatments greatly augmented the degree of liver injury in LXRα$^{-/-}$ mice (Fig. 1C and Supporting Fig. S1C). Serum ALT and aspartate aminotransferase (AST) activities were marginally enhanced in LXRα$^{-/-}$ mice (24 hours after last CCl_4 injection) (Fig. 1D). In a separate experiment, serum ALT activities were significantly increased 72 hours after the last CCl_4 injection (Fig. 1E). These results show that LXRα activation may protect hepatocytes from toxicant-induced injury.

LXRα PROTECTION OF HEPATOCYTES FROM TGF-β

To understand how LXRα protects hepatocytes, we analyzed gene-expression profiles in the liver of LXR$^{-/-}$ mice using the Gene Expression Omnibus (GEO) database (GSE38083) available in the public domain (Supporting Fig. S2A). Pathway analysis using the Kyoto Encyclopedia of Genes and Genomes database enabled us to find lipid metabolism pathways enriched in down-regulated differentially expressed genes (DEGs) (Supporting Fig. S2B). In up-regulated DEGs, pathways associated with inflammation were enriched (Supporting Fig. S2C). In the network analysis using the Mentha database, TGF-β receptors (TβRI and TβRII) were found in the core network of up-regulated DEGs (Supporting Fig. S2D), suggestive of LXRα as a molecule that may regulate TGF-β signaling.

To validate an association between LXRα and TGF-β, we determined the effects of TGF-β1 and other inflammatory cytokines (i.e., interleukin-6 [IL-6] or TNF-α) on LXRα and found that only TGF-β1 has an inhibitory effect on LXRα (Fig. 2A, upper). This effect was confirmed in a time-course study (Fig. 2A, lower). In addition, treatment of mouse primary hepatocytes with TGF-β1 caused a decrease in *Nr1h3* (LXRα) mRNA level, which was antagonized by LXRα agonist treatment (Fig. 2B). More importantly, cell death induced by TGF-β1 was abrogated by concomitant LXRα agonist treatment (Fig. 2C). The cytoprotective effect of LXRα against TGF-β1 was corroborated by fluorescence-activated cell sorting analysis (Fig. 2D). Likewise, GW3965 reversed changes in apoptosis and survival biomarker levels (Fig. 2E). Akt is used to indicate hepatocyte viability, as it is suppressed

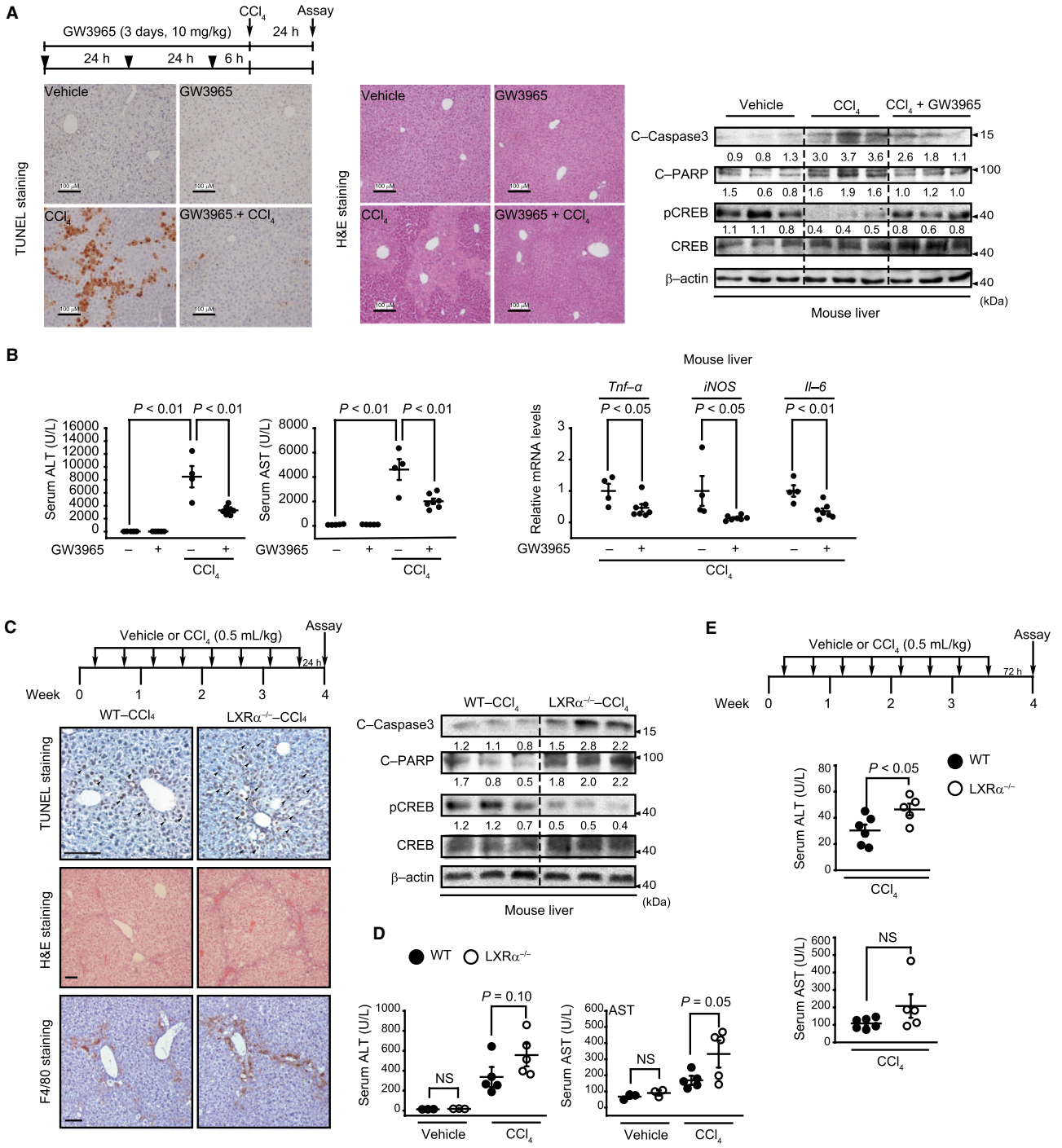

FIG. 1. Protection of liver cells by LXRα from injurious stimuli. (A) Assays for hepatocyte apoptosis. TUNEL and hematoxylin and eosin staining were carried out for the liver sections (scale bar = 100 μm) from C57BL/6 mice (n = 4-7 per group, male). Immunoblottings were done on liver homogenates. (B) Serum ALT and AST activities and quantitative RT-PCR assays for inflammatory cytokines. (C) Assays for hepatocyte apoptosis. WT or LXRα$^{-/-}$ mice were injected with CCl_4 for indicated times (n = 3 or 5 per group, female) and sacrificed 24 hours after last CCl_4 injection. TUNEL-positive cells were indicated with arrowheads. Scale bar = 100 μm. (D) Serum ALT and AST activities in mice treated as in (C). (E) Serum ALT and AST activities at 72 hours after last CCl_4 injection (n = 5 or 6 per group, female). For (A) and (C), values represent fold changes relative to control. Quantification was normalized to β-actin. For (B), (D), and (E), data represent the mean ± SEM (statistical difference was determined by two-tailed Student *t* test). Abbreviations: h, hours; H&E, hematoxylin and eosin; iNOS, inducible nitric oxide synthase; and NS, not significant.

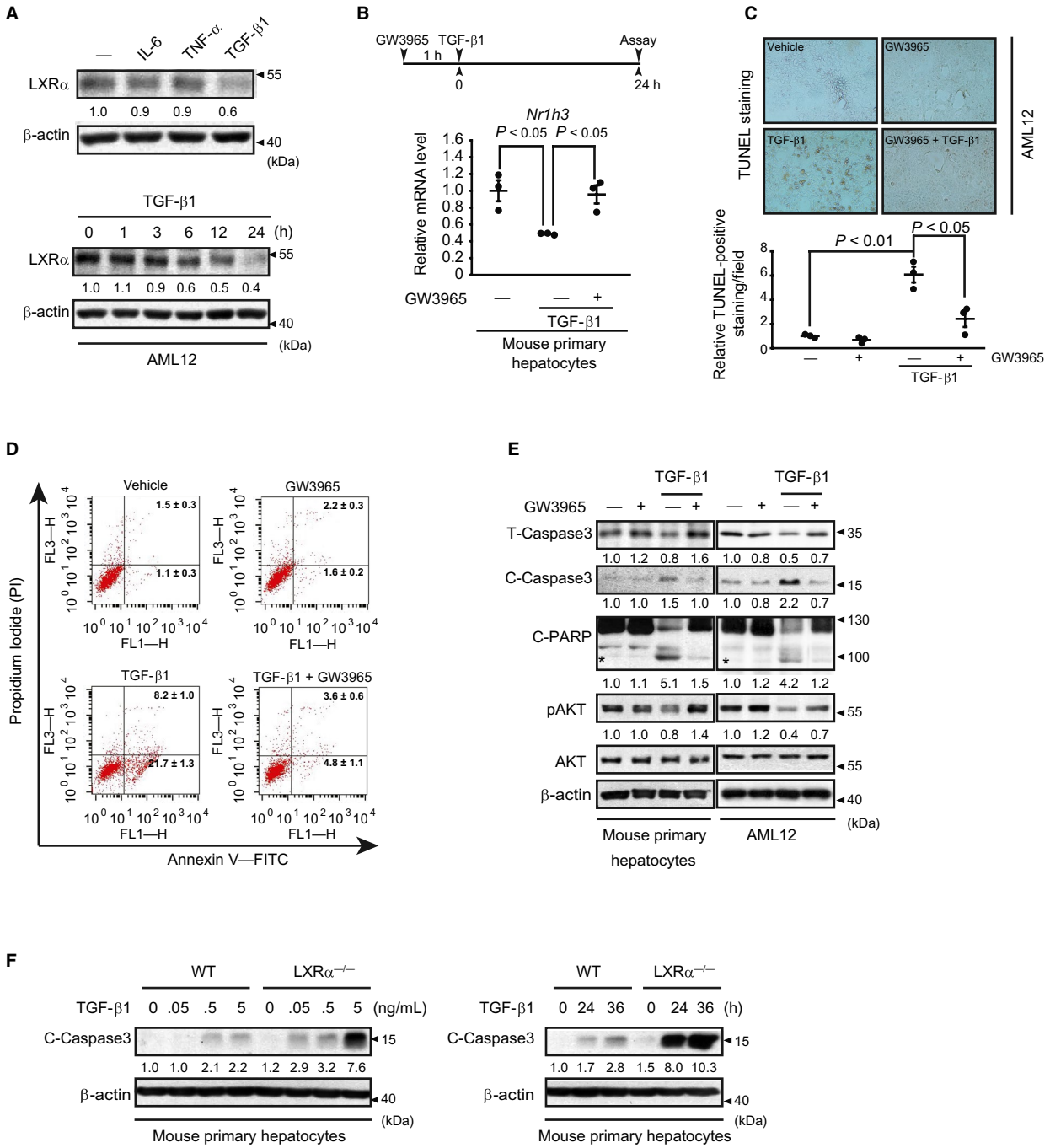

FIG. 2. Inhibition of TGF-β1-induced hepatocyte death by LXRα. (A) Immunoblottings for LXRα in cells treated with 50 ng/mL IL-6, 60 ng/mL TNF-α, or 5 ng/mL TGF-β1 for 24 hours or with 5 ng/mL TGF-β1 for indicated times. (B) Quantitative RT-PCR assays for *Nr1h3* (LXRα). Mouse primary hepatocytes were treated with 3 μM GW3965 for 1 hour and continuously exposed to 5 ng/mL TGF-β1 for 24 hours (n = 3 isolations, male). (C) TUNEL staining. The cells were treated as in (B) (n = 3 replicates). (D) Flow cytometric analyses for fluorescein isothiocyanate–annexin V and propidium iodide in cells treated as in (B). Values represent the mean ± SEM of three independent experiments. (E) Immunoblottings in cells treated as in (B). (F) Immunoblottings for C-caspase3. Hepatocytes prepared from WT or LXRα$^{-/-}$ mice were treated with TGF-β1 for 24 hours (left panel) or 5 ng/mL TGF-β1 for the indicated times (right panel). For (A), (E), and (F), multiple assays were done (n = 3), and representative blots were shown. Values represent fold changes relative to control. For (B) and (C), data represent the mean ± SEM (statistical difference was determined by two-tailed Student *t* test). Abbreviations: FITC, fluorescein isothiocyanate; and h, hours.

in oxidative stress-induced liver injury[10]; thus, Akt activator protects hepatocytes from apoptosis and alleviates endotoxin-induced liver injury.[11] As expected, GW3965 treatment prevented decrease of p-Akt (Fig. 2E). Moreover, a deficiency in LXRα markedly increased TGF-β1-induced cleaved caspase-3 in primary hepatocytes (Fig. 2F). These results show that LXRα may protect hepatocytes from TGF-β.

CO-REPRESSION OF CB2 AND LXRα UNDER CONDITIONS OF LIVER INJURY

Having identified the hepatocyte-protecting effect of LXRα against TGF-β, we next explored the downstream molecule(s) regulated by LXRα. First, gene-expression patterns were analyzed using a public GEO database (GSE25583).[12] Genes expressed with similar response patterns after treatment with single (1-day) or double (1-week) doses of CCl_4 were clustered and categorized (Fig. 3A). The hierarchical cluster closest to LXRα contained 21 genes. Of them, *Nr1h3* (LXRα), *As3mt* (arsenic, +3 oxidation state, methyltransferase), *Acads* (acyl-coenzyme A dehydrogenase, short chain), *Tek* (TEK receptor tyrosine kinase), *Cnr2* (CB2), *F5* (coagulation factor V), and *Dhcr24* (24-dehydrocholesterol reductase) were related to the "response to stress/stimulus" term (marked with violet circles). In quantitative RT-PCR assays on primary hepatocytes isolated from mice treated with a single dose of CCl_4, the mRNA levels of *Nr1h3*, *Cnr2*, and *Dhcr24* (a neuroprotective LXRα target gene[13]) were markedly diminished (Fig. 3B, upper). *As3mt*, *F5*, *Tek*, and *Acads* mRNA levels varied (Supporting Fig. S3). Of note, *Nr1h3* and *Cnr2* transcript levels strongly correlated with each other (Fig. 3B, lower). In the analyses of GEO databases from livers of patients with hepatitis/cirrhosis (GSE20140) or mice with concanavalin A-induced hepatitis (GSE17184), significant correlations existed between LXRα and CB2 (Fig. 3C). We further determined their levels in human samples. In this approach, nontumorous liver tissues adjacent to liver cancer were collected and classified into portal fibrosis, septal fibrosis, and cirrhosis according to the severity of fibrosis stage. We observed gradual decreases in LXRα protein levels as liver fibrosis worsened; LXRα protein levels were significantly lower in the septal fibrosis and cirrhosis groups than the portal fibrosis group (Fig. 3D, left). Consistently, LXRα levels negatively correlated with those of alpha-smooth muscle actin (α-SMA, a fibrosis marker) (Supporting Fig. S4). In addition, CB2 mRNA levels were decreased in the septal fibrosis or cirrhosis groups (Fig. 3D, middle), indicative of CB2 repression in parallel with LXRα as liver fibrosis worsened. A significant correlation also existed between LXRα protein and CB2 transcript levels (Fig. 3D, right).

CB2 EXPRESSION IN HEPATOCYTES AND ITS CYTOPROTECTIVE ROLE

We next examined the role of CB2 in hepatocytes in liver protection. Because the Kupffer cell is a major liver cell type expressing CB2, we used a clodronate-mediated macrophage depletion model and assessed the effect of CB2 agonist JWH133 on CCl_4-induced liver injury. As expected, JWH133 treatment exerted a hepatoprotective effect (Fig. 4A,B, and Supporting Fig. S5A). We found that CCl_4-induced liver injury was not ameliorated by concomitant clodronate treatment, despite successful macrophage depletion, which was validated using F4/80 (Egf-like module containing, mucin-like, hormone receptor-like 1) staining and quantitative RT-PCR assays (Supporting Fig. S5B,C). Of note, JWH133 treatment effectively protected the liver from CCl_4 plus clodronate treatment (Fig. 4A,B, and Supporting Fig. S5A), confirmative of the cytoprotective effect of CB2 in hepatocytes.

CB2 transcripts have two splicing variants, namely, *Cnr2a* (NM_009924.4) and *Cnr2b* (NM_001305278.1).[14] Immunoblotting for CB2 suffers from the lack of specificity of commercially available primary antibodies.[14] Thus, we applied quantitative RT-PCR analyses and carefully designed several different primers for CB2 and its variants to validate CB2 expression in hepatocytes (Supporting Fig. S6A). Total *Cnr2, Cnr2a,* and *Cnr2b* were all expressed in the liver of C57BL/6 mice (spleen was used as positive control) (Supporting Fig. S6A). Moreover, *Cnr2* and its variants *Cnr2a* and *Cnr2b* were all expressed in the hepatocytes (Supporting Fig. S6B, left). As compared with the nonparenchymal cell fraction, total *Cnr2* levels as assessed using

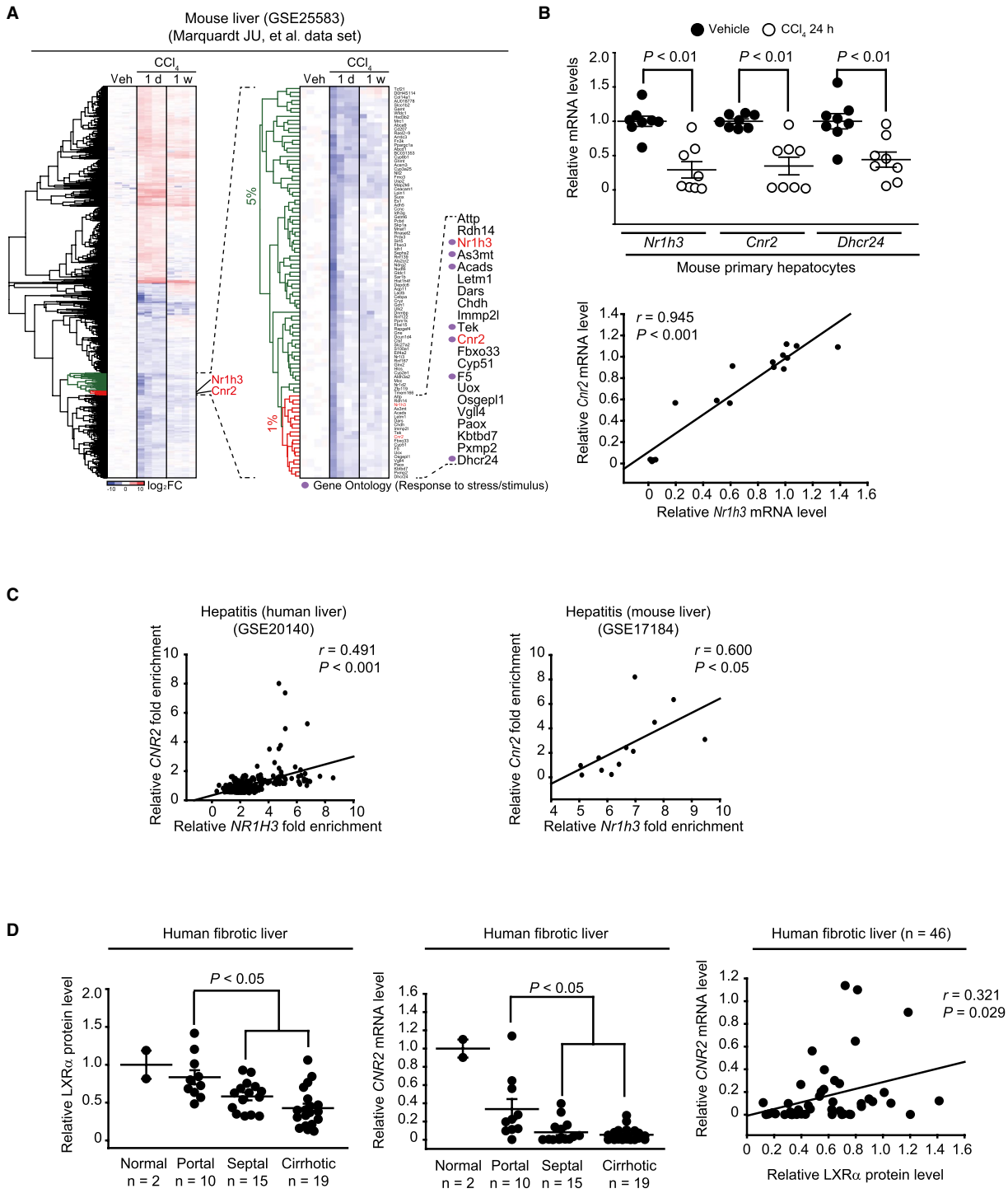

FIG. 3. LXRα and CB2 repression under the conditions of liver injury. (A) Heat map and hierarchical correlation analyses of the genes in the complementary DNA microarray obtained from GSE25583. Genes with expressional relevance to LXRα are indicated by the red (the cluster comprising 1% genes) corresponding region in the dendrogram. (B) Quantitative RT-PCR assays for *Nr1h3* (LXRα) and relevant genes in hepatocytes isolated from mice 24 hours after treatment with vehicle or CCl_4 (n = 4 per group, male, 2 replicates for each mouse) and correlation of *Nr1h3* (LXRα) and *Cnr2* (CB2). (C) Correlation between LXRα and CB2 in patients with hepatitis (GSE20140, n = 307) and in the liver of mice with hepatitis (GSE17184). (D) LXRα protein levels and quantitative RT-PCR assays for *CNR2* in patient liver specimens. For (B)-(D), coefficients were obtained using the Pearson analysis; for (B) and (D), data represent the mean ± SEM (statistical difference was determined by two-tailed Student *t* test. Abbreviation: h, hours.

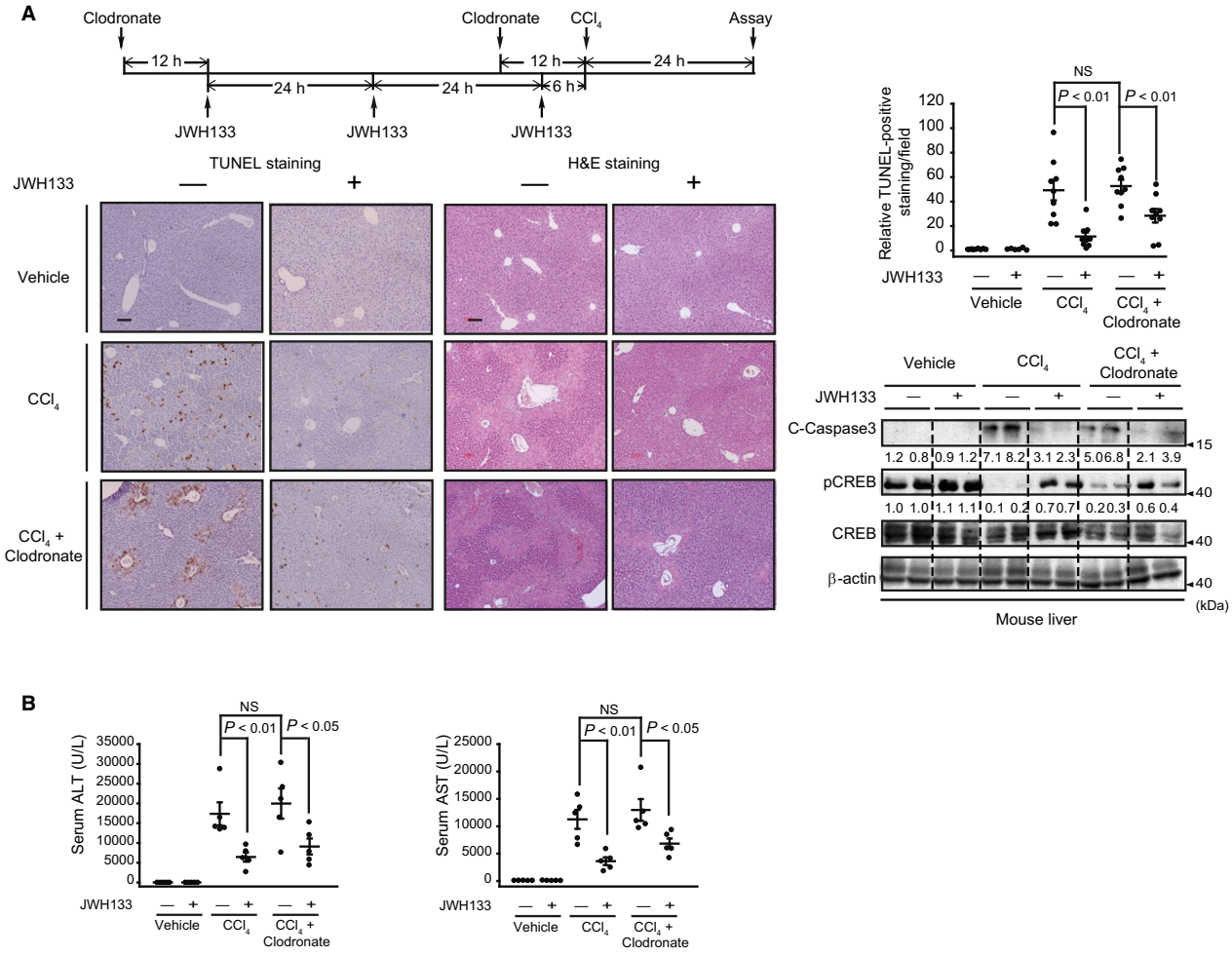

FIG. 4. The role of CB2 in hepatocytes in the protection of liver. (A) The hepatoprotective effect of JWH133 in C57BL/6 mice treated with CCl_4 and clodronate. Mice were treated with JWH133 (10 mg/kg body weight per day), clodronate (100 μL/mice), and CCl_4, as shown in the scheme (n = 5 per group, male). Relative TUNEL positivity was assessed from two or three samples per condition (two samples for JWH133 alone and three samples for the others, randomly selected from five samples), and three random fields per sample were evaluated. Scale bar = 100 μm. (B) Serum ALT and AST activities in mice treated as previously. For (A) and (B), data represent the mean ± SEM (statistical difference was determined by two-tailed Student *t* test). For (A), values represent fold changes relative to control. Abbreviations: h, hours; and NS, not significant.

different primers were approximately 35% in hepatocytes; *Cnr2a* and *Cnr2b* levels were approximately 15% and 50%, respectively (Supporting Fig. S6B, left). In hepatocytes, *Cnr2b* transcript levels were higher than *Cnr2a* transcript levels (Supporting Fig. S6B, right). The purity of isolated hepatocytes was validated by RT-PCR assays for cell-type-specific markers in hepatocytes and nonparenchymal cell fraction (Supporting Fig. S6C). Consistently, GW3965 treatment increased *Cnr2a* and *Cnr2b* mRNA levels (Supporting Fig. S6D). To corroborate CB2 presence in hepatocytes, we validated the CB2 pathway using protein kinase A (PKA)-mediated enzymatic assay. Because CB2 activation leads to inhibition of adenylyl cyclase and thereby PKA activity through $G_{i/o}$ protein coupling,[15] PKA activity was measured using immunoblotting for phospho-PKA substrate; JWH133 treatment decreased PKA activity, which was entirely reversed by CB2 knockdown (Supporting Fig. S6E). These results provide evidence that hepatocytes express functionally active CB2 downstream of LXRα.

TRANSCRIPTIONAL INDUCTION OF CB2 BY LXRα

To assess the effect of LXRα on CB2, we determined whether LXRα agonist treatment induces CB2 using animal and cell models. Treatment of mice with GW3965 enhanced the hepatic *Cnr2* level (Fig. 5A). Similarly, GW3965 increased *Cnr2* in both mouse primary hepatocytes and alpha mouse liver 12 (AML12) cells (Fig. 5A). We hypothesized that LXRα transcriptionally up-regulates *Cnr2* by binding to LXR response elements (LXREs) in the gene. Of the three putative LXRE motifs found in the CB2 gene promoter, GW3965 treatment increased LXRα occupancy at LXRE2 but not LXRE1 or LXRE3 (Fig. 5B). We then made an LXRE2 mutant promoter construct containing the −1.4-kb upstream region of CB2 gene for luciferase assays and found that LXRα activation failed to increase luciferase expression from the mutant construct (Fig. 5C). Together, these results showed that LXRα transcriptionally regulates CB2 gene expression.

Subsequently, we explored the causal relationship between CB2 induction and TGF-β antagonism by LXRα. JWH133 treatment inhibited TGF-β1-induced cleavage of caspase-3 in AML12 cells (Fig. 5D, left). SR144528, a CB2 inverse agonist, attenuated the inhibitory effect of LXRα on the caspase-3 cleavage

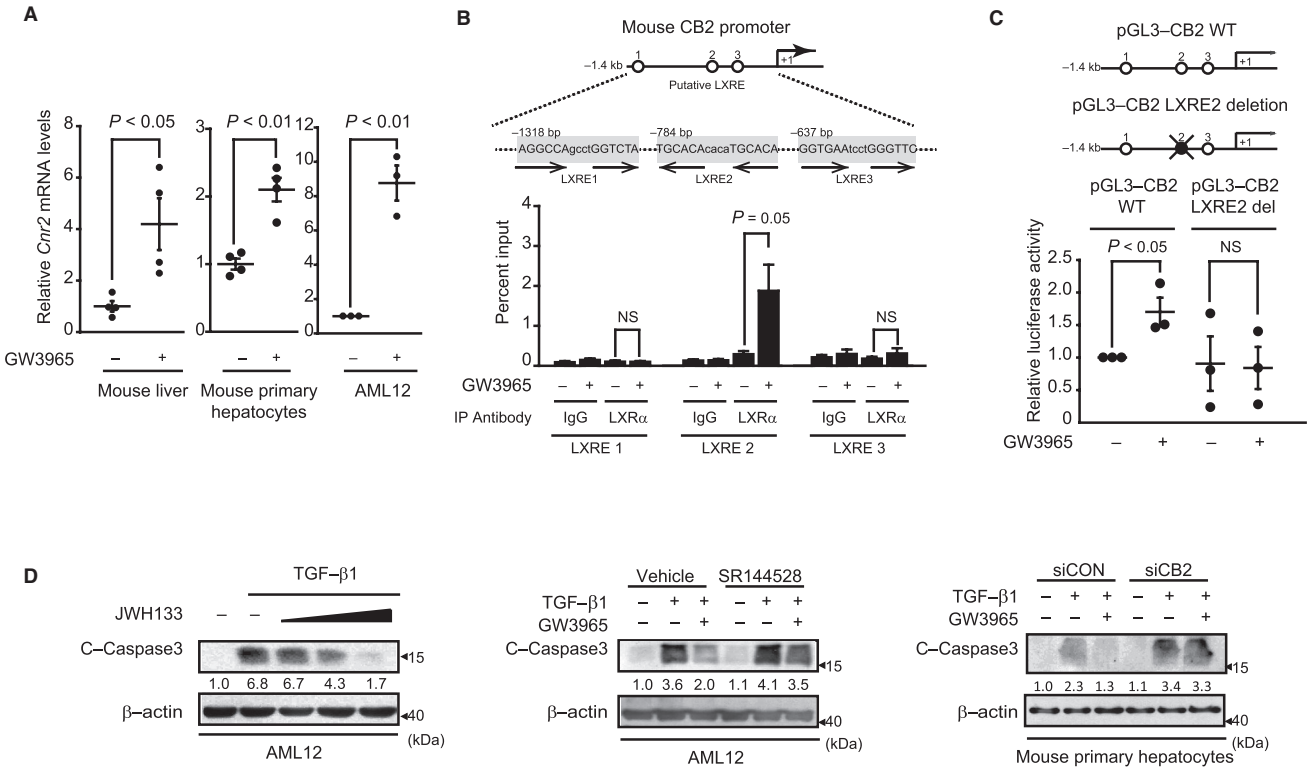

FIG. 5. Transcriptional induction of CB2 by LXRα. (A) Quantitative RT-PCR assays for *Cnr2* in the liver of mice (n = 4 per group, male) treated with GW3965 (3 mg/kg body weight per day) for 3 days (left) or in mouse primary hepatocytes (middle, n = 4 isolations, male) and AML12 cells (right) treated with GW3965 (3 μM, 24 hours). (B) Chromatin immunoprecipitation assays for LXRα binding to the promoter region of CB2 gene. Quantitative PCR assays were done for quantification. (C) Promoter reporter assays using pGL3-CB2 or its LXRE2 deletion mutant construct. AML12 cells were transfected with each construct (1 μg, 24 hours) and then treated with vehicle or GW3965 (3 μM, 12 hours). (D) Immunoblotting for C-caspase3. AML12 cells were treated with JWH133 (1, 3, and 10 μM for 1 hour) and continuously exposed to 5 ng/mL TGF-β1 for 24 hours (left). The cells were also treated with 3 μM GW3965 for 1 hour after 4 μM SR144528 treatment for 30 minutes and continuously exposed to TGF-β1 (middle). Mouse primary hepatocytes were similarly treated with GW3965 and TGF-β1 after small interfering RNA (siRNA) knockdown for 48 hours (right). For (A)-(C), data represent the mean ± SEM of three separate experiments (statistical difference was determined by two-tailed Student *t* test). For (D), multiple assays were done (n = 3), and representative blots are shown. Values represent fold changes relative to control. Abbreviations: bp, base pair; IgG, immunoglobulin G; IP, immunoprecipitation; and NS, not significant.

(Fig. 5D, middle). Likewise, CB2 knockdown resulted in a similar outcome in primary hepatocytes (Fig. 5D, right). Hence, it is highly likely that the cytoprotective effect of LXRα against TGF-β relies on CB2 expression in hepatocytes.

TβRI INHIBITION BY CB2, AS MEDIATED BY MIR-27B-DEPENDENT INHIBITION OF USP4

Next, we studied how CB2 induced by LXRα inhibits TGF-β signaling. Attention was paid to ubiquitin modification of TβRI, an upstream molecule sensing TGF-β signal. Intriguingly, GW3965 activation of LXRα facilitated ubiquitination of TβRI in AML12 cells (Fig. 6A, left). LXRα activation destabilized TβRI in the experiment using cycloheximide (Fig. 6A, middle). Moreover, SR144528 treatment prevented GW3965 from inhibiting TβRI (Fig. 6A, right). To understand the role of the LXRα-CB2 pathway for TβRI destabilization, we assessed USP4 that fortifies TGF-β signaling by acting as a deubiquitylating enzyme for TβRI.[16] As expected, treatment of hepatocytes with either GW3965 or JWH133 decreased USP4 levels (Fig. 6B, left). Moreover, SR144528 treatment abrogated the inhibitory effect of LXRα on USP4 (Fig. 6B, middle). Consistently, USP4 overexpression diminished the cytoprotective effect of GW3965 against TGF-β1 (Fig. 6B, right). Our results indicate that LXRα induction of CB2 may contribute to TβRI destabilization in hepatocytes through USP4 inhibition.

With the aim of identifying the molecule responsible for USP4 inhibition, we focused on the regulatory effect of miRNA because we previously observed that miR-148a directly inhibits USP4 in hepatocellular carcinoma.[17] In a preliminary study, CB2 activation by JWH133 failed to alter miR-148a level (data not shown), prompting us to consider other candidates. Therefore, we analyzed the miRNAs down-regulated in the liver of mice treated with CCl_4 (for 1, 4, and 8 weeks)[18] and extracted eight USP4-targeting candidates using a prediction software tool (microRNA.org) (Fig. 6C, left and middle). Among them, miR-27b was significantly enhanced by CB2 agonist treatment (Fig. 6C, right). In the analysis of human liver specimens, miR-27b levels were substantially lower in patients with septal fibrosis or cirrhosis than those with portal fibrosis and correlated with CB2 levels (Fig. 6D). In cell-based assays, LXRα agonist treatment increased miR-27b, and this effect was entirely prevented by either SR144528 treatment or CB2 knockdown (Fig. 6E), confirmative of LXRα/CB2 regulation of miR-27b.

To verify the direct inhibitory effect of miR-27b on USP4, USP4 3′-UTR-luciferase activity assays were done. MiR-27b mimic transfection prevented luciferase expression from Luc-USP4-3′-UTR construct, whereas its inhibitor transfection had the opposite effect (Fig. 6F, left). Modulations of the miRNA with mimic or antisense oligonucleotide (ASO) appropriately changed USP4 levels (Fig. 6F, right). Finally, miR-27b ASO transfection antagonized the inhibitory effect of CB2 agonist (Fig. 6G), verifying the ability of miR-27b to inhibit USP4 downstream from CB2.

PROTECTION OF HEPATOCYTES FROM INJURY BY LIVER-SPECIFIC DELIVERY OF LXRα

To verify the function of LXRα on hepatocyte injury and regulation of the targets *in vivo*, we used an albumin promoter–driven lentiviral LXRα delivery system (LV-LXRα^{alb}) to reinstate LXRα expression in the liver of LXRα$^{-/-}$ mice and subjected them to repetitive injuries. Quantitative RT-PCR assays confirmed LXRα increase by LV-LXRα^{alb} delivery (Supporting Fig. S7A). As expected, LV-LXRα^{alb} infection diminished TUNEL staining intensities and injury assessed by histopathology of hematoxylin and eosin in LXRα$^{-/-}$ mice treated with multiple doses of CCl_4 (Fig. 7A, left). The protective effect of LXRα on hepatocytes was corroborated by alterations in apoptosis and cell survival biomarkers (Fig. 7A, right); LV-LXRα^{alb} delivery tended to decrease serum ALT activities ($P = 0.1$) (Supporting Fig. S7B) and to increase *Cnr2* mRNA level ($P = 0.06$) (Fig. 7B, upper); miR-27b level significantly increased (Fig. 7B, upper). Consistently, USP4 and TβRI levels were decreased (Fig. 7B, lower). LXRα overexpression in hepatocytes lessened the transcripts of hepatic inflammatory cytokines (Fig. 7C). Moreover, enforced expression of LXRα attenuated liver fibrosis, as shown by the results of Masson's trichrome staining and immunoblottings for α-SMA, fibronectin, and collagen 1a1 (Fig. 7D).

In a separate experiment, we confirmed not only LXRα overexpression after LV-LXRα^{alb} delivery using

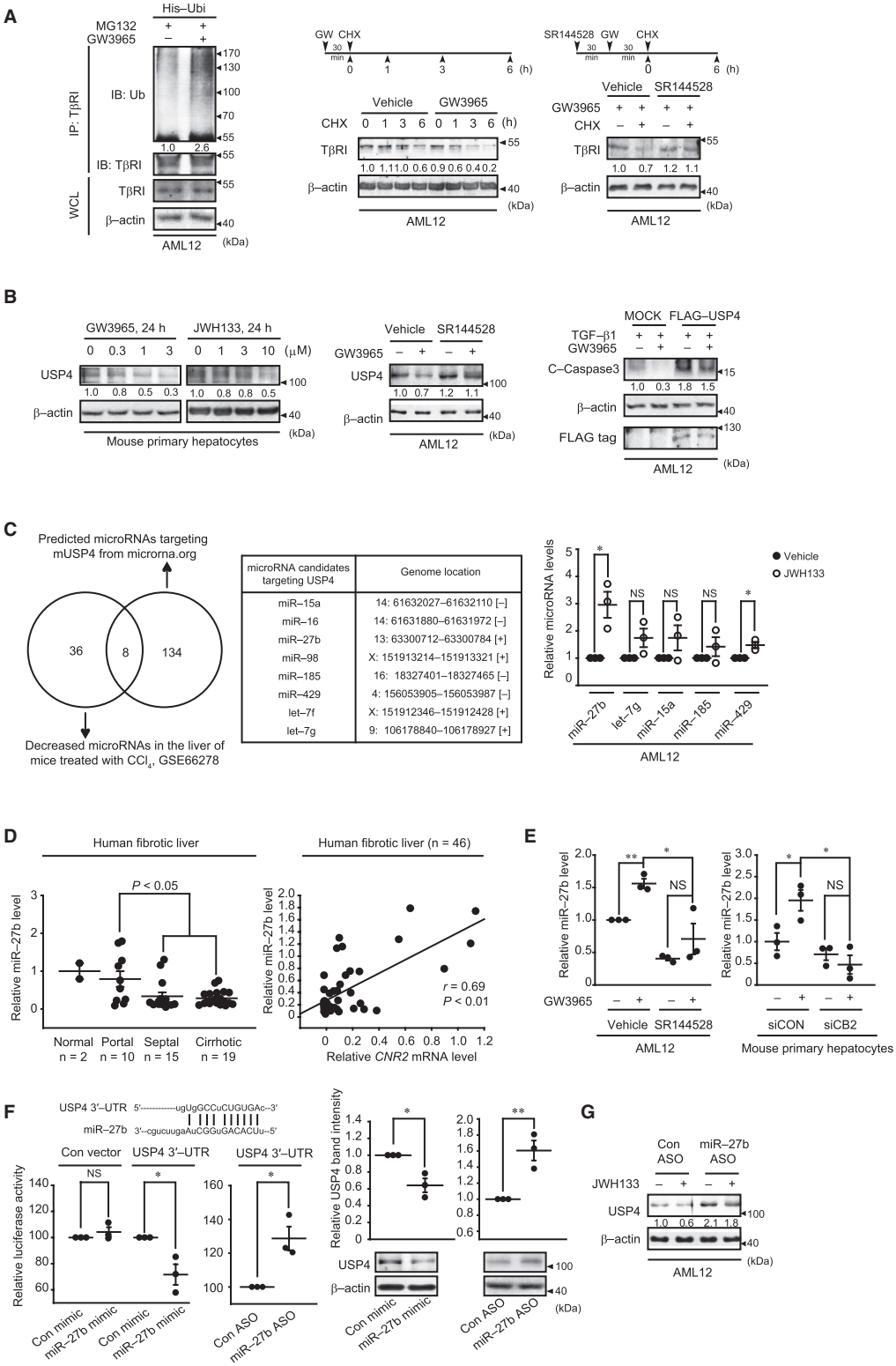

quantitative RT-PCR assays (Supporting Fig. S7C) but also inhibition of liver injury in the liver of WT or LXRα$^{-/-}$ mice (Supporting Fig. S7D). Increases of *Cnr2* mRNA and miR-27b were also verified (Supporting Fig. S7E). Consistently, USP4, TβRI, and α-SMA protein levels were all decreased (Supporting

FIG. 6. USP4 repression by miR-27b downstream of LXRα and CB2. (A) TβRI stability in AML12 cells treated with GW3965 (3 μM, 24 hours) after transfection with His-tagged ubiquitin (His-Ubi). MG132 (10 μM) was added 6 hours before cell lysis (left). The cells were treated with GW3965, SR144528 (4 μM), and cycloheximide (CHX, 20 μg/mL) as indicated (middle and right). (B) Immunoblottings for USP4 and C-caspase3. Primary hepatocytes were treated with GW3965 or JWH133 (left); AML12 cells were treated with SR144528 (30 minutes) and continuously exposed to GW3965 (24 hours) (middle) or treated with GW3965 and TGF-β1 after transfection with FLAG-tagged USP4 (1 μg, 24 hours) (right). (C) miRNA candidates targeting USP4. A Venn diagram and table show an overlapping of decreased miRNAs in the liver of mice treated with CCl_4 (GSE66278) and those predicted to target mouse USP4 (microRNA.org). Quantitative RT-PCR assays for the miRNAs in AML12 cells treated with JWH133 (10 μM, 24 hours). (D) Quantitative RT-PCR assays for miR-27b in human specimens and correlation analysis. (E) Quantitative RT-PCR assays for miR-27b in AML12 cells treated with SR144528 (30 minutes) and continuously exposed to GW3965 (24 hours) or in mouse primary hepatocytes treated with GW3965 after transfection of CB2 siRNA (or control siRNA) for 48 hours. (F) USP4 3′-UTR reporter and USP4 immunoblotting assays in AML12 cells transfected with mock or miR-27b mimic (or ASO). (G) USP4 immunoblots in AML12 cells treated with JWH133 (24 hours) after miR-27b ASO transfection (48 hours). For (A), (B), and (G), multiple assays were done (n = 3), and representative blots are shown. Values represent fold changes relative to control. For (C), (E), and (F), data represent the mean ± SEM of three separate experiments (statistical difference was determined by two-tailed Student *t* test, $^{*}P < 0.05$, $^{**}P < 0.01$). Abbreviations: CHX, cycloheximide; h, hours; IB, immunoblotting; IP, immunoprecipitation; min, minutes; NS, not significant; Ub, ubiquitin; and WCL, whole cell lysates.

Fig. S7F). Our results show that LXRα protects hepatocytes from TGF-β-induced injury by CB2, as mediated by increase of miR-27b for the inhibition of USP4 and TβRI (Fig. 7E).

ACETAMINOPHEN-INDUCED LIVER INJURY MODEL

Because acetaminophen (APAP) overdose highly contributes to drug-induced liver injury in human, and APAP-induced liver injury was associated with activation of TGF-β signaling,[19,20] we assessed whether inhibition of TGF-β signaling ameliorates APAP-induced apoptosis. Either SB525334 (a TβRI inhibitor) treatment or TβRII knockdown prevented an increase in C-caspase3 level (Supporting Fig. S8A), suggestive of the role of TGF-β receptor signaling in APAP-induced apoptosis. We then analyzed LXRα (*NR1H3*) and LXRβ (*NR1H2*) transcript levels using GEO databases and found that APAP treatment decreased *LXRα* but not *LXRβ* mRNA levels in HepaRG cells (a hepatic progenitor cell line with characteristics of human hepatocyte) and rat primary hepatocytes (Supporting Fig. S8B). In the database, the up-regulated or down-regulated genes were analyzed. The top four enriched pathways were obtained from the DEGs using the DAVID program (Supporting Fig. S8C, upper). A core network existed in the highly interconnected region, including LXRα, USP4, and TGFBR1 (Supporting Fig. S8C, lower). We further examined the effect of a toxic dose of APAP on the targets in mice and found that APAP intoxication indeed repressed hepatic LXRα, with increases of USP4 and TβRI and decreases of *Cnr2* mRNA and miR-27b levels (Supporting Fig. S8D). GW3965 posttreatments inhibited hepatocyte injury against an APAP challenge (Supporting Fig. S8E, left and middle). Moreover, GW3965 treatment also prevented APAP from decreasing the LXRα mRNA level (Supporting Fig. S8E, right). All of these results showed the beneficial effect of LXRα in the treatment of acute liver injury.

Discussion

Our findings demonstrate that LXRα activation protects hepatocytes from injury, supporting the concept that either ligand activation or genetic overexpression of LXRα exerted a beneficial effect on hepatocyte viability. In patients with fatty liver and nonalcoholic steatohepatitis, however, LXRα is overexpressed in hepatocytes, culminating in excessive triglyceride accumulation.[7] Hence, the outcome shown in the present study is quite distinct from that observed in nonalcoholic fatty liver disease characterized by LXRα overexpression.

Our results demonstrate that LXRα prevents hepatocyte apoptosis through inhibition of TGF-β signaling. Therefore, LXRα knockout augmented TGF-β cytotoxicity. Moreover, TGF-β in turn down-regulated LXRα. Thus, LXRα and TGF-β may act against each other in an antagonistic manner for hepatocyte viability, supportive of the loop pathway between LXRα and TGF-β. It has also been shown that TGF-β was elevated in mice treated with CCl_4 or APAP[20,21] and in patients with acute liver

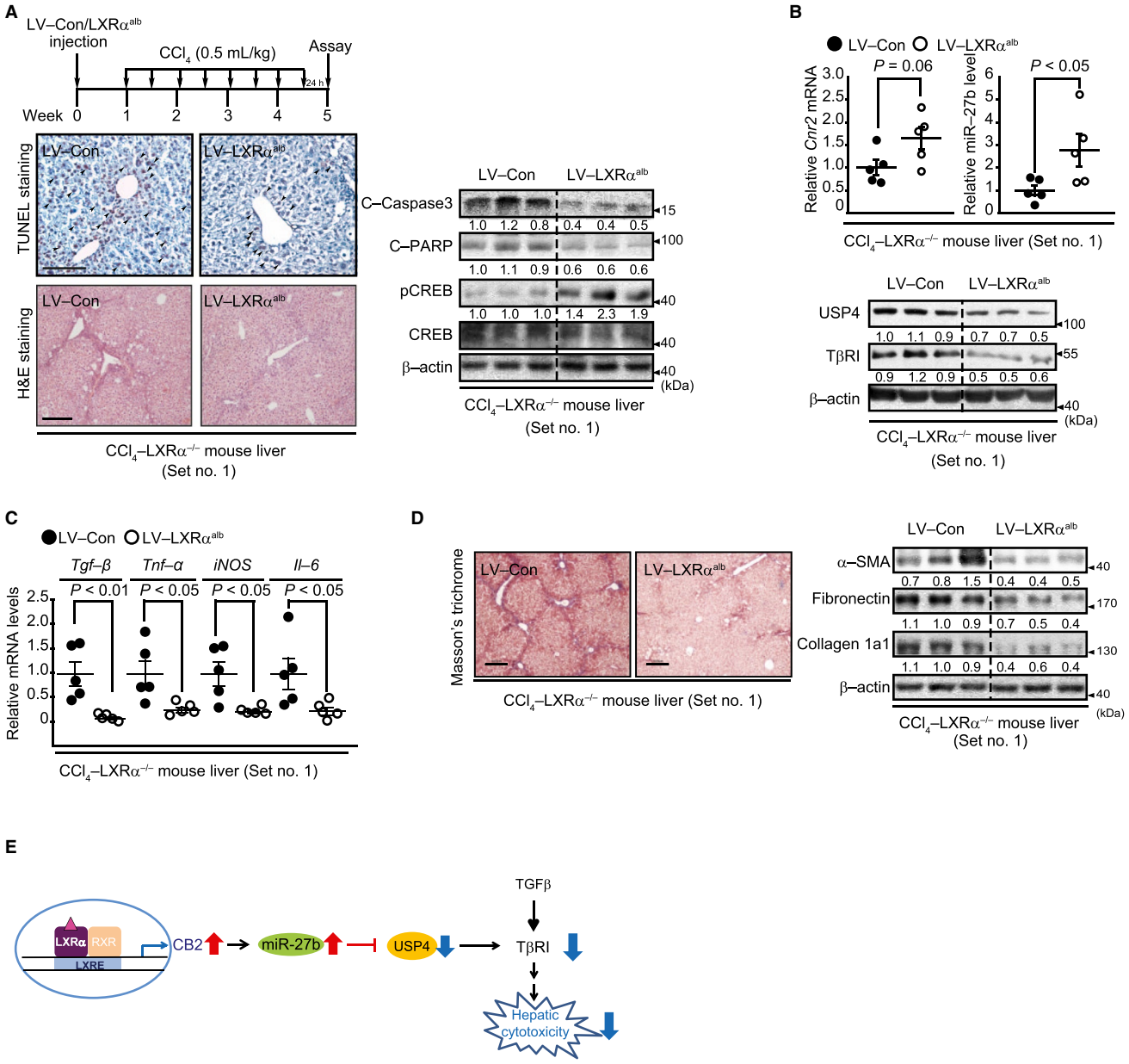

FIG. 7. Amelioration of hepatocyte injury by liver-specific overexpression of LXRα. (A) Assays for hepatocyte apoptosis. WT or LXRα$^{-/-}$ mice (n = 5 per group, female) were injected with lentiviruses that express control (LV-Con) or LXRα (LV-LXRα^{alb}) for 7 days and subjected to CCl_4 treatments for 4 weeks. TUNEL-positive cells were indicated with arrowheads. Scale bar = 100 μm. (B) Quantitative RT-PCR assays for *Cnr2* and miR-27b and immunoblottings for USP4 and TβRI. (C) Quantitative RT-PCR assays for inflammatory cytokines. (D) Masson's trichrome stainings and immunoblottings for fibrosis markers. Scale bar = 100 μm. (E) A schematic illustrating the proposed mechanism by which LXRα protects hepatocytes from TGF-β-induced injury. For (A), (B), and (D), values represent fold changes relative to control. For (B) and (C), data represent the mean ± SEM (statistical difference was determined by two-tailed Student *t* test). Abbreviations: alb, albumin promoter; Con, control; h, hours; and LV, lentiviral.

failure.[20,22] Given the lack of information on the role of TGF-β signaling in toxicant-induced liver injury, we additionally performed an experiment using SB525334, an inhibitor of TβRI, and found that SB525334 treatment ameliorated CCl_4-induced liver injury, as shown by decreases in serum ALT activity and hepatic *Bax* mRNA level (Supporting Fig. S9). The data are consistent with the report that either

TβRI inhibitor treatment or genetic deletion of TβRI caused a faster recovery from toxicant-induced liver injury.[20] Hence, inhibition of TGF-β may be of value in the therapy of acute liver injury.

Analysis of the DEGs in the liver of $LXR^{-/-}$ mice available in the public GEO database (GSE38083) enabled us to find TGFBR2 and TGFBR1 as a link in the core network. TNF-α, a well-studied multifunctional cytokine that regulates various cellular processes, showed both protective and damaging effects at the same time in CCl_4-induced acute injury.[23] However, we did not find any clue related to TNF-α signaling in this analysis. Moreover, GW3965 had no protective effect on AML12 cell apoptosis induced by TNF-α plus cycloheximide (data not shown). Our findings and others support the idea that the liver-protecting effect of LXRα may result from the inhibition of TGF-β but not TNF-α.

LXRα primarily manages cholesterol homeostasis in the liver, whereas LXRβ may regulate energy balance in organs such as brain and skeletal muscle.[24,25] In the present study, CCl_4 treatment decreased the transcript levels of LXRα (*Nr1h3*) but not LXRβ (*Nr1h2*) in an *ex vivo* experiment using hepatocytes (Fig. 3B and Supporting Fig. S10A). Similarly, treatment of hepatocytes with TGF-β1 caused a decrease in *Nr1h3* mRNA, as reversed by LXRα agonist treatment (Fig. 2B); *Nr1h2* mRNA was unaffected by TGF-β1 and/or GW3965 treatment (Supporting Fig. S10B), despite the expectation of both LXRα and LXRβ activation by GW3965.[5] Hence, it is highly likely that LXRα but not LXRβ contributes primarily to protecting hepatocytes from TGF-β.

Attention has been paid to the development of the CB2 receptor as a therapeutic target, particularly for liver diseases.[26,27] Nevertheless, chemical agonists of CB2 have fared poorly in clinic trials due to the fact that they have affinities for CB1 and thus produce CB1-mediated unwanted effects.[15] Thus, efforts should be made to better understand CB2 regulation and identify the appropriate target(s). Our data demonstrate that LXRα regulates CB2 in hepatocytes. Moreover, the liver-protecting effect of $LV\text{-}LXR\alpha^{alb}$ was reversed by treatment with SR144528 (a CB2 inverse agonist) (Supporting Fig. S11), strengthening the functional role of CB2 in the LXRα effect.

Existence of CB2 in hepatocytes has been debated. Some studies have confirmed CB2 expression in mouse hepatocytes,[28,29] whereas others insisted on lack of CB2 expression in hepatocytes.[30] The results from our quantitative RT-PCR assays, however, supported the notion that *Cnr2* is indeed expressed in hepatocytes, although the expression level is lower than that in nonparenchymal cell fraction. Furthermore, this study identified *Cnr2a* and *Cnr2b* expression in hepatocytes. In our model using different primers, we also found the lack of *Cnr2a* presence in hepatocytes when we used primers set No. 4, the same ones used in the previous study insisting on the absence of *Cnr2* in hepatocytes.[30] However, application of different primer sets enabled us to detect *Cnr2a* transcript. Moreover, both *Cnr2a* and *Cnr2b* variants were inducible by LXRα agonist in hepatocytes. The functional relevance of CB2 in hepatocytes was corroborated by the outcome of PKA-dependent activity assay.

MiR-27b regulates cancer development by serving as a tumor suppressor or oncogene.[31,32] Our study identifies miR-27b as an inhibitor of USP4. This molecular link is associated with USP4-dependent TGF-β signaling. MiR-27b works as an antifibrotic miRNA in pulmonary fibroblasts and may be enhanced by TGF-β to positively regulate the endothelial-mesenchymal transition.[33,34] Hence, our results and others support an miRNA-dependent feedback loop pathway for TGF-β signaling.

Drug-induced liver injury is a worldwide health problem and is the most common type of hepatocyte death.[19] The effects of APAP intoxication on our targets of interest were corroborated in the present study. Moreover, our finding supports the view that post-treatment with LXRα agonist may have a potential beneficial effect for the treatment of acute liver injury. Overall, this study uncovers a CB2-dependent pathway in hepatocytes downstream from LXRα, elaborating on targets and strategies for the prevention and potential cure of TGF-β-mediated hepatocyte injury.

REFERENCES

1) Racanelli V, Rehermann B. The liver as an immunological organ. Hepatology 2006;43:S54-S62.
2) Malhi H, Guicciardi ME, Gores GJ. Hepatocyte death: a clear and present danger. Physiol Rev 2010;90:1165-1194.
3) Takehara T, Tatsumi T, Suzuki T, Rucker EB, Hennighausen L, Jinushi M, et al. Hepatocyte-specific disruption of Bcl-xL leads to continuous hepatocyte apoptosis and liver fibrotic responses. Gastroenterology 2004;127:1189-1197.
4) Inokuchi S, Aoyama T, Miura K, Osterreicher CH, Kodama Y, Miyai K, et al. Disruption of TAK1 in hepatocytes causes hepatic

injury, inflammation, fibrosis, and carcinogenesis. Proc Natl Acad Sci U S A 2010;107:844-849.
5) Kohro T, Nakajima T, Wada Y, Sugiyama A, Ishii M, Tsutsumi S, et al. Genomic structure and mapping of human orphan receptor LXR alpha: upregulation of LXRa mRNA during monocyte to macrophage differentiation. J Atheroscl Thromb 2000;7:145-151.
6) Peet DJ, Turley SD, Ma W, Janowski BA, Lobaccaro JM, Hammer RE, et al. Cholesterol and bile acid metabolism are impaired in mice lacking the nuclear oxysterol receptor LXR alpha. Cell 1998;93:693-704.
7) **Schultz JR**, **Tu H**, Luk A, Repa JJ, Medina JC, Li L, et al. Role of LXRs in control of lipogenesis. Genes Dev 2000;14:2831-2838.
8) Zhu W, Jia Q, Wang Y, Zhang Y, Xia M. The anthocyanin cyanidin-3-O-beta-glucoside, a flavonoid, increases hepatic glutathione synthesis and protects hepatocytes against reactive oxygen species during hyperglycemia: involvement of a cAMP-PKA-dependent signaling pathway. Free Radic Biol Med 2012;52:314-327.
9) **Li J**, **Dou X**, **Li S**, Zhang X, Zeng Y, Song Z. Nicotinamide ameliorates palmitate-induced ER stress in hepatocytes via cAMP/PKA/CREB pathway-dependent Sirt1 upregulation. Biochim Biophys Acta 2015;1853:2929-2936.
10) Zeng T, Zhang CL, Zhao N, Guan MJ, Xiao M, Yang R, et al. Impairment of Akt activity by CYP2E1 mediated oxidative stress is involved in chronic ethanol-induced fatty liver. Redox Biol 2018;14:295-304.
11) **Jing ZT**, **Liu W**, Xue CR, Wu SX, Chen WN, Lin XJ, et al. AKT activator SC79 protects hepatocytes from TNF-alpha-mediated apoptosis and alleviates d-Gal/LPS-induced liver injury. Am J Physiol Gastrointest Liver Physiol 2019;316:G387-G396.
12) Marquardt JU, Seo D, Gomez-Quiroz LE, Uchida K, Gillen MC, Kitade M, et al. Loss of c-Met accelerates development of liver fibrosis in response to CCl(4) exposure through deregulation of multiple molecular pathways. Biochim Biophys Acta 2012;1822:942-951.
13) Wang Y, Rogers PM, Stayrook KR, Su C, Varga G, Shen Q, et al. The selective Alzheimer's disease indicator-1 gene (Seladin-1/DHCR13) is a liver X receptor target gene. Mol Pharmacol 2008;74:1716-1721.
14) Li Y, Kim J. Neuronal expression of CB2 cannabinoid receptor mRNAs in the mouse hippocampus. Neuroscience 2015; 311:253-267.
15) Dhopeshwarkar A, Mackie K. CB2 Cannabinoid receptors as a therapeutic target-what does the future hold? Mol Pharmacol 2014;86:430-437.
16) **Zhang L**, **Zhou F**, Drabsch Y, Gao R, Snaar-Jagalska BE, Mickanin C, et al. USP4 is regulated by AKT phosphorylation and directly deubiquitylates TGF-beta type I receptor. Nat Cell Biol 2012;14:717-726.
17) Heo MJ, Kim YM, Koo JH, Yang YM, An J, Lee SK, et al. microRNA-148a dysregulation discriminates poor prognosis of hepatocellular carcinoma in association with USP4 overexpression. Oncotarget 2014;5:2792-2806.
18) **Knabel MK**, **Ramachandran K**, Karhadkar S, Hwang HW, Creamer TJ, Chivukula RR, et al. Systemic delivery of scAAV8-encoded MiR-29a ameliorates hepatic fibrosis in carbon tetrachloride-treated mice. PLoS One 2015;10:e0124411.
19) Suk KT, Kim DJ. Drug-induced liver injury: present and future. Clin Mol Hepatol 2012;18:249-257.
20) Bird TG, Muller M, Boulter L, Vincent DF, Ridgway RA, Lopez-Guadamillas E, et al. TGFbeta inhibition restores a regenerative response in acute liver injury by suppressing paracrine senescence. Sci Transl Med 2018;10:eaan1230.
21) Niu L, Cui X, Qi Y, Xie D, Wu Q, Chen X, et al. Involvement of TGF-beta1/Smad3 signaling in carbon tetrachloride-induced acute liver injury in mice. PLoS One 2016;11:e0156090.
22) **Antoniades CG**, **Quaglia A**, **Taams LS**, Mitry RR, Hussain M, Abeles R, et al. Source and characterization of hepatic macrophages in acetaminophen-induced acute liver failure in humans. Hepatology 2012;56:735-746.
23) **Dong Y**, **Liu Y**, **Kou X**, Jing Y, Sun K, Sheng D, et al. The protective or damaging effect of Tumor necrosis factor-alpha in acute liver injury is concentration-dependent. Cell Biosci 2016;6:8.
24) Quinet EM, Savio DA, Halpern AR, Chen L, Schuster GU, Gustafsson JA, et al. Liver X receptor (LXR)-beta regulation in LXRalpha-deficient mice: implications for therapeutic targeting. Mol Pharmacol 2006;70:1340-1349.
25) Miao Y, Wu W, Dai Y, Maneix L, Huang B, Warner M, et al. Liver X receptor beta controls thyroid hormone feedback in the brain and regulates browning of subcutaneous white adipose tissue. Proc Natl Acad Sci U S A 2015;112:14006-14011.
26) **Louvet A**, **Teixeira-Clerc F**, Chobert MN, Deveaux V, Pavoine C, Zimmer A, et al. Cannabinoid CB2 receptors protect against alcoholic liver disease by regulating Kupffer cell polarization in mice. Hepatology 2011;54:1217-1226.
27) Munoz-Luque J, Ros J, Fernandez-Varo G, Tugues S, Morales-Ruiz M, Alvarez CE, et al. Regression of fibrosis after chronic stimulation of cannabinoid CB2 receptor in cirrhotic rats. J Pharmacol Exp Ther 2008;324:475-483.
28) **Suk KT**, **Mederacke I**, Gwak GY, Cho SW, Adeyemi A, Friedman R, et al. Opposite roles of cannabinoid receptors 1 and 2 in hepatocarcinogenesis. Gut 2016;65:1721-1732.
29) Hall D, Poussin C, Velagapudi VR, Empsen C, Joffraud M, Beckmann JS, et al. Peroxisomal and microsomal lipid pathways associated with resistance to hepatic steatosis and reduced pro-inflammatory state. J Biol Chem 2010;285:31011-31023.
30) **Deveaux V**, **Cadoudal T**, **Ichigotani Y**, Teixeira-Clerc F, Louvet A, Manin S, et al. Cannabinoid CB2 receptor potentiates obesity-associated inflammation, insulin resistance and hepatic steatosis. PLoS One 2009;4:e5844.
31) Matsuyama R, Okuzaki D, Okada M, Oneyama C. MicroRNA-27b suppresses tumor progression by regulating ARFGEF1 and focal adhesion signaling. Cancer Sci 2016;107:28-35.
32) **Sun XF**, **Sun JP**, Hou HT, Li K, Liu X, Ge QX. MicroRNA-27b exerts an oncogenic function by targeting Fbxw7 in human hepatocellular carcinoma. Tumour Biol 2016;37:15325-15332.
33) Zeng X, Huang C, Senavirathna L, Wang P, Liu L. miR-27b inhibits fibroblast activation via targeting TGFbeta signaling pathway. BMC Cell Biol 2017;18:9.
34) Suzuki HI, Katsura A, Mihira H, Horie M, Saito A, Miyazono K. Regulation of TGF-beta-mediated endothelial-mesenchymal transition by microRNA-27. J Biochem 2017;161:417-420.

Author names in bold designate shared co-first authorship.

Supporting Information

Additional Supporting Information may be found at onlinelibrary.wiley.com/doi/10.1002/hep4.1415/suppinfo.